1-2015

Thermodynamic Grain Size Stabilization Models: An Overview

Mostafa Saber
Portland State University, msaber@pdx.edu

Carl C. Koch
North Carolina State University

Ronald O. Scattergood
North Carolina State University

MATERIALS RESEARCH LETTERS

Mater. Res. Lett., 2015
Vol. 3, No. 2, 65–75, http://dx.doi.org/10.1080/21663831.2014.997894

Taylor & Francis
Taylor & Francis Group

www.tandfonline.com/toc/tmrl20/current

Thermodynamic Grain Size Stabilization Models: An Overview

Mostafa Saber*, Carl C. Koch and Ronald O. Scattergood

Department of Materials Science and Engineering, North Carolina State University, 911 Partners Way, Room 3002, Raleigh, NC 27695-7907, USA

(*Received 17 June 2014; final form 8 December 2014*)

Grain boundaries in a nanocrystalline microstructure produce an increase in the excess free energy of the system. Grain growth is a consequence of the thermodynamic driving force reducing this excess. Thermodynamic stabilization is an approach based on eliminating the driving force by suitable alloy additions that can produce a metastable equilibrium state at the nanoscale grain size, as opposed to kinetic stabilization where the grain growth mobility is restricted by pinning and/or drag mechanisms. The present paper reviews and compares various models proposed for thermodynamic stabilization.

Keywords: Grain Growth, Nanocrystalline Materials, Grain Boundary Segregation, Thermal Stability

Introduction The processing–structure–property relationships in nanocrystalline materials have been a focus of many studies. The processing variables to synthesize nanocrystalline materials, such as temperature, pressure, and atmosphere, impact the structure and properties. Enhanced properties of nanocrystalline materials are attributed to their unique microstructure. For instance, nanoscale grains improve the mechanical behavior such that the strength (or hardness) is increased to an extent unattainable by the micron-scale counterpart.[1,2]

There are various methods to generate nanoscale microstructures. These techniques mostly incorporate severe plastic deformation (SPD), extremely rapid solidification, or gas-phase condensation.[1,2] The use of inert gas condensation (IGC) was the early work developed by Gleiter.[3] These methods are typically divided into bottom-up and top-down approaches. Typical bottom-up methods are IGC,[3,4] and electrodeposition (ED) methods.[5–7] The top-down techniques are high-pressure torsion (HPT),[8–13] equal channel angular pressing,[14–19] and high-energy ball milling (BM).[20–30]

SPD techniques such as high-energy BM are capable of providing a metastable microstructure with nanoscale grains.[1] A large amount of grain boundary within the microstructure leads to an increase in the Gibbs excess free energy. Reduction in this excess free energy provides a driving force for returning to a more stable state, which will be the coarsened microstructure. This driving force can cause drastic grain growth in nanocrystalline materials when the temperature is increased. This effect has been studied for many pure nanocrystalline metals, which often show extensive grain growth at low homologous temperature.[1,31]

There are two approaches with which thermal stabilization of a nanoscale grain size has been explained. The first is the kinetic mechanism, which reduces mobility of the grain boundaries, but does not eliminate excess free energy driving force. The second is the thermodynamic mechanism based on the metastable equilibrium such that the driving force for grain growth would be eliminated at a critical grain size. A primary requirement for grain size stabilization in both approaches is the presence of solute additions within the microstructure. If a suitable solute addition is added, the excess free energy driving force for grain growth can be eliminated and thermodynamic stabilization at higher temperatures will be attained. Solute additions also contribute to kinetic stabilization effects such as solute drag, second phase particle pinning, and chemical ordering that reduce grain mobility.

There is rarely any direct evidence to describe which stabilization mechanisms are effective in a given alloy and the question still remains: how to predict the operative mechanisms in thermally stable nanocrystalline alloy systems. To answer this question, various

*Corresponding author. Email: msaber@ncsu.edu

analytical models have been developed.[32] These models will be reviewed in the present paper. This review aims to provide insights into thermodynamic aspects of stabilization in nanocrystalline materials.

Background The reduction of excess interface Gibbs free energy G with increasing solute content can be described by the Gibbs adsorption isotherm[33]

$$d\gamma = -\Gamma \, \mathrm{d}\mu, \tag{1}$$

where μ is the chemical potential of the solute atom dissolved in a matrix of solvent atoms. Γ represents the excess amount of solute atoms segregated to the boundary. Plots of $\gamma = \mathrm{d}G/\mathrm{d}A$ versus global solute concentration obtained by Hondros and Seah [34] show a reduction of γ with increasing solute concentration. This negative trend is intensified for solute atoms with large atomic size misfit. This effect suggests that large non-equilibrium atomic size misfit solutes can segregate to grain boundaries and consequently could reduce excess grain boundary free energy with the possible outcome of grain size stabilization at $\gamma = 0$. γ is not to be confused with grain boundary cohesive energy. The concept was developed further in the solution models proposed by Weissmüller,[35,36] Kirchheim and coworkers,[37–39] and Darling et al.[40] These models are applied in the dilute solution limit. Trelewicz and Schuh [41] proposed a binary mixing model applicable to non-dilute solutions with finite grain boundary volume fraction, but they did not include the elastic strain energy enthalpy change due to solute elastic size misfit. Saber et al. [42,43] modified this approach to include elastic enthalpy, and subsequently extended it to the wider class of ternary alloy systems. In addition to this, nanostructured alloy stability diagrams and atomistic modeling simulations relevant to grain boundary stabilization by alloy addition have been reported.

Gibb's adsorption isotherm in Equation (1) cannot be integrated directly unless the relation between Γ and μ is known. This not known for most cases and various approaches have been adopted to obtain solutions. The results for thermodynamic stabilization models for binary alloys often appear in a typical form, albeit with modifications related to assumptions such as the dilute solution limit and fully saturated grain boundaries. A simple rationalization of this form can be made using Figure 1 where the total grain boundary interface area A is represented by the closed domain. n_i and n_b are solute concentrations in the grain boundary interface and bulk matrix, respectively.

If G is the excess Gibbs free energy due to grain boundary interface area A at fixed T, P, and n_i, the change $\mathrm{d}G$ to extend the grain boundary interface area by $\mathrm{d}A$ into bulk matrix would be

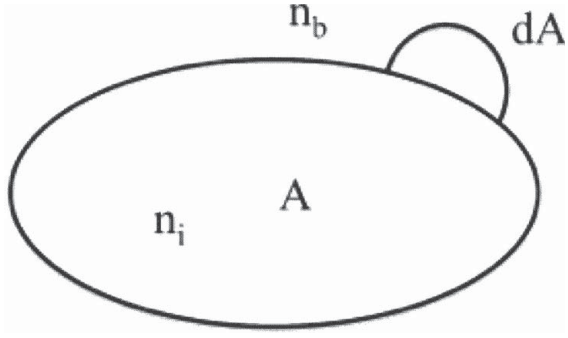

Figure 1. Variation in dA grain boundary area A for solute concentrations indicated.

$$\begin{aligned} \mathrm{d}G &= \left(\frac{\partial G}{\partial A}\right)_{T,P,n_b} \mathrm{d}A + \left(\frac{\partial G}{\partial n}\right)_{T,P,A} \mathrm{d}n, \\ \frac{\mathrm{d}G}{\mathrm{d}A} &= \left(\frac{\partial G}{\partial A}\right)_{T,P,n_b} + \frac{\mathrm{d}n}{\mathrm{d}A}\left(\frac{\partial G}{\partial n}\right)_{T,P,A}, \\ \gamma &= \gamma_0 + \Gamma \Delta G_\mathrm{seg}. \end{aligned} \tag{2}$$

The first term in $\mathrm{d}G$ is the variation to extend the grain boundary interface into the bulk matrix at concentration n_b and the second term is the variation $\mathrm{d}G$ needed to increase the solute concentration in dA from n_b to n_i. The converse effect for grain shrinkage would have the same form with appropriate changes in sign. ΔG_seg represents the solute segregation free energy change, Γ represents the grain boundary solute excess and γ_0 would correspond to the grain boundary energy of pure solvent, but only in the dilute solution limit $n_\mathrm{b} \to 0$. Various sign conventions have been used which could change the sign of the $\Gamma \Delta G_\mathrm{seg}$ term. The metastable equilibrium for thermodynamic stabilization is possible when $\gamma = 0$. In the case of metastable equilibrium for non-dilute solutions where $n_\mathrm{b} > 0$, the remaining solute would be subjected to additional reaction such as precipitation.

McLean [44] defined the enthalpy of segregation ΔH_seg as the complete release of the elastic strain energy ΔH_els associated with solute atomic size misfit. On the other hand, Defay et al. [45] defined the enthalpy of segregation in terms of chemical (bond energy) contributions ΔH_chem. However, it was pointed out that neither the model of McLean nor the model of Defay et al. individually give a comprehensive model of the grain boundary segregation since each of these models consider only one of these two possible contributions.[46]

The total enthalpy of segregation is given in the Wynblatt–Ku approximation [47] as a linear combination of these two contributions

$$\Delta H_\mathrm{seg} = \Delta H_\mathrm{chem} + \Delta H_\mathrm{els}. \tag{3}$$

For discussion purposes, the Wynblatt–Ku approximation is defined in the sense that the total segregation enthalpy would be the linear sum of the chemical and elastic contributions; no specific model for these is implied unless indicated. Wynnblatt and Chatain [48] give an extensive review of interfacial segregation models. Based on regular solution theory, the chemical enthalpy contribution ΔH_{chem} for a binary solid solution can be described in terms of the near neighbor bond energies of solute and solvent atoms within the grain or within grain boundaries. The elastic enthalpy of segregation ΔH_{els} is the released elastic strain energy ΔE_{els} per solute atom when transferred to the grain boundary. Using a model due to Friedel,[49] the elastic part can be obtained as

$$\Delta H_{\text{els}} = -\Delta E_{\text{els}} = \frac{2K_{\text{B}}G_{\text{A}}(V_{\text{B}} - V_{\text{A}})^2}{3K_{\text{B}}V_{\text{A}} + 4G_{\text{A}}V_{\text{B}}}, \qquad (4)$$

where K is the bulk modulus, G is the shear modulus, and V is the molar volume. A or B are the solute or solvent, respectively. The emphasis for models discussed in the following sections will be on the approach rather than detailed analysis with derivations and equations.

Model Proposed by Weissmüller This follows Cahn's approach [33] in applying the general Gibbs interface equation. In Weissmüller's treatment, the dependence of grain boundary properties on crystal orientation and on curvature is neglected. This is also the case for all subsequent models discussed in this review. The model proposed was based on a dilute solution limit and the derived equation has the form [35,36]

$$\gamma = \gamma_0 - \{N_{\text{i}}\}^{\text{sat}}(\Delta H_{\text{seg}} + RT\ln x_b), \qquad (5)$$

where γ_0 is the energy of non-segregated grain boundary interface in the dilute solution approximation and $\{N_{\text{i}}\}^{\text{sat}}$ is the solute excess for fully saturated grain boundary interface. ΔH_{seg} is the segregation enthalpy and $RT\ln x_{\text{b}}$ represents the ideal mixing entropy for bulk solute concentration x_{b}. It was shown that if γ is negative in the coarse-grain limit, there exists a value of grain size where $\gamma = 0$, which would then represent the metastable state for grain size stabilization. Results for selected values of the parameters in Equation (5) imply that the grain size at stabilization decreases as the solute content increases at a fixed temperature. These basic trends were prelude to further development of thermodynamic stabilization models by later investigators, as discussed next.

It should be noted that grain growth at elevated temperatures is considered at a closed system of polycrystal. Therefore, the driving force for grain growth is defined as the variation of the Gibbs free energy with respect to the variation of grain boundary area at a constant temperature and pressure. Consequently, an equation for the specific grain boundary energy in an alloy is obtained. Equation (5) provides a useful form of the grain boundary energy for the special case of a binary alloy where the alloy is considered as a dilute solution. In the thermodynamic equilibrium state, where $\mathrm{d}G/\mathrm{d}A = 0$, the solute concentrations in the matrix and grain boundaries are related by an adsorption isotherm. The enthalpy of segregation, ΔH_{seg}, ideally involves the chemical energy contribution due to the chemical interaction of solute–solvent and the elastic strain energy contribution due to the atomic size misfit. This equation is employed to define thermodynamic stabilization as the condition where γ is reduced to be zero. Hereafter, γ represents the excess free energy associated with non-equilibrium solute in solution. If $\gamma = 0$ is assumed to be cohesive grain boundary energy, grain boundary cohesion would be eliminated. It should be emphasized that the definition of excess grain boundary energy in Equation (5) is limited to a dilute solution containing a negligible volume fraction of interface. These boundary conditions are in contrast with nanocrystalline microstructures in which the volume fraction of grain boundary is significant.

Models Proposed by Kirchheim et al. The analysis due to Weismuller was extended by Kirchheim [37] to include the temperature dependence of grain size for a metastable equilibrium state. The equilibrium grain size as a function of temperature was obtained by combining the value for segregation enthalpy with the entropy for an ideal dilute solution with fully saturated grain boundaries $\Gamma = \Gamma_{\text{sat}}$ and a value for the pure solvent grain boundary energy γ_0

$$\gamma = \gamma_0 + \Gamma_{\text{sat}}[RT\ln x - \Delta H_{\text{seg}}]. \qquad (6)$$

The grain size was introduced using mass conservation for the solute atoms and a monolayer of fully saturated grain boundary with spherical grains was used.

The grain diameter at saturation (the equilibrium grain size) for an alloy with high segregation enthalpy and negligible solute solubility limit can be obtained as [38]

$$D = \frac{3\Gamma_E^* V_{\text{AB}}}{X_{\text{A}}^0}, \qquad (7)$$

where Γ_{s}^* is the solute excess equivalent of a saturated grain boundary monolayer, X_{A}^0 is the summation of the bulk and interface solute concentration, and V_{AB} is the molar volume of the alloy. This equation shows that if the solute content is increased, the equilibrium grain size becomes smaller. The result is an implicit equation for grain size that in the general case must be solved numerically.

In a saturated grain boundary, there is a competition between precipitation and segregation. If the empirical relation for strongly segregating solute atoms is

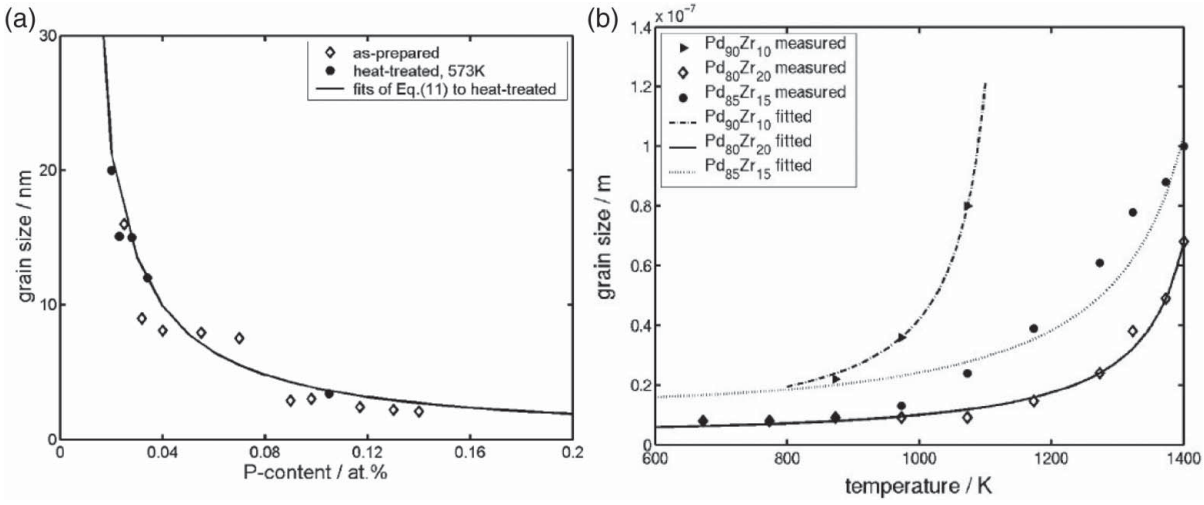

Figure 2. (a) Grain size vs. % P for Ni–P at 300°C.[39] (b) Grain size vs. T for Pd–Zr alloys.[39]

employed from [37], it is shown that precipitation can ultimately result in a lower energy state.

Estimating values for ΔH_{seg}, and γ_0 for NiP and RuAl, the plots of inverse grain size vs. $\ln T$, where temperature T reveals a linear trend.[37] Liu and Kircheim [38,39] extended this approach to analyze results for ball-milled PdZr alloys, using the dilute solution approximation with fully saturated grain boundaries and best fit values of γ_0, Γ_{sat}, and ΔH_{seg} in Equation (6). The results also showed a linear trend for inverse grain size vs. $\ln T$. Alternatively, results can be plotted as grain size vs. solute content at a fixed temperature as shown in Figure 2(a), or grain size vs. temperature for different solute contents as shown in Figure 2(b). This latter type of plot is a useful measure of the thermodynamic mechanism potential for grain size stabilization at elevated temperature in a given alloy system over a range of solute addition. It is also useful for comparing model results for a given alloy system between different investigators and different modeling approaches. The Zr solute contents in Figure 2(b) range up to 20 at.%. At these high solute concentrations the results may not be consistent with a dilute solution approximation. This can also be the case for NiP alloys in Figure 2(a) with P content up to 12 at.%. The authors considered the trends to be reasonable approximations for thermodynamic stabilization.

Model Proposed by Darling et al. Using a thermodynamic analysis based on simultaneous internal processes, Darling et al. [40] derived an equation for $\gamma = dG/dA$. The binary regular solution model bond energy parameters and the elastic size misfit for ΔH_{seg} were introduced using the Wynblatt–Ku approximation. The grain boundary was assumed to be a bilayer interface including in-plane and out-of -plane bonds. The chemical term ΔH_{chem} is a modification of the Defray surface monolayer regular solution model that includes the inter-grain boundary bonds across the bilayer interface.[48] The resulting equation is again in the form of Equation (1). The chemical and elastic enthalpy parameters needed for evaluation are available in an extensive database.[50] Similar to models proposed by Kirchheim and coworkers,[37–39] mass balance for the solute is introduced along with the ΔH_{seg} and ΔS_{seg} relations. An implicit equation for γ must be solved numerically. Results can be obtained for γ vs. grain boundary mol fraction x^{GB}_{solute} curves for a range of grain sizes at a fixed annealing temperature as shown in Figure 3(a) for FeZr alloys. It was assumed that γ_0 in Equation (1) is the grain boundary energy of the pure solvent; that is, a dilute solution approximation. Thermodynamic stabilization is obtained at the grain size where the γ curves first intersect zero as shown in Figure 3(a) (red symbols for $d = 23.1$ nm). If not kinetically hindered, negative values of γ would lead to grain size decrease to the metastable state. Extending this procedure over a range of temperatures and solute content produces grain size vs. temperature plots for FeZr alloys in Figure 3(b). It can be noted that corresponding plots of inverse grain size vs. $\ln T$ for the results in Figure 3(b) would show significant curvature, in contrast to results in [37–39]. A form of grain size stability map was also produced by these authors, as will be discussed in a later section. It must also be noted that although this model incorporates the effect of elastic enthalpy due to the atomic size misfit into the regular solution model, it would not simultaneously minimize the regular solution Gibbs free energy with respect to all the variables. This model uses the derivative with respect to the solute content at a constant volume fraction of grain boundary (constant grain size) and finds the equilibrium point, however, the grain boundary volume fraction is not constrained to remain constant while segregation occurs.

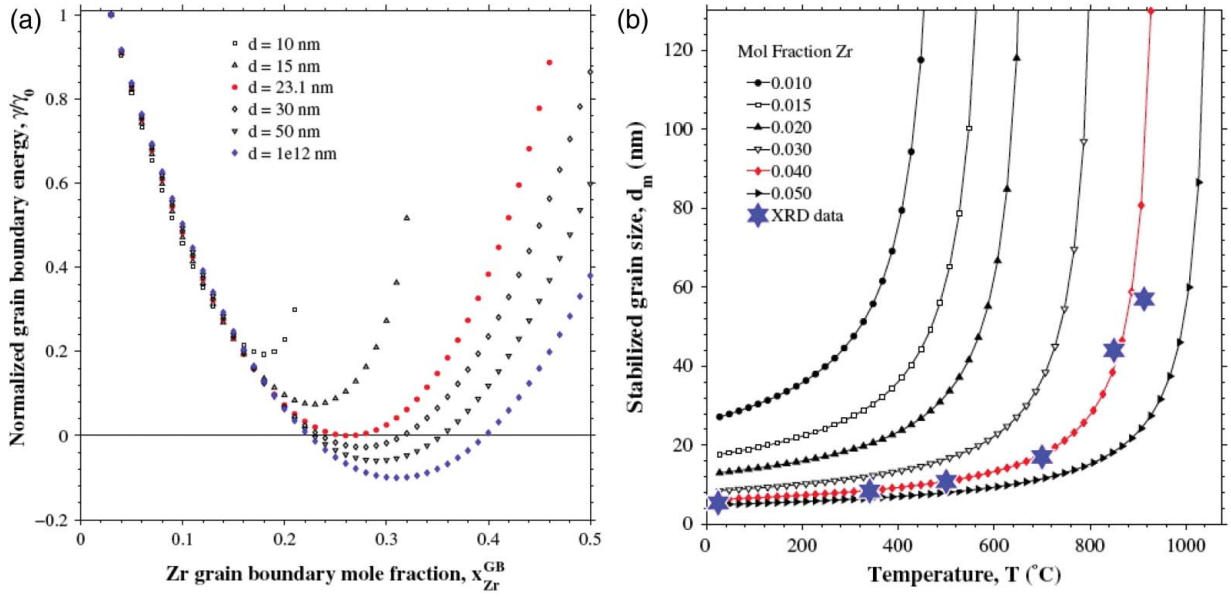

Figure 3. (a) γ/γ_0 vs. x_{Zr}^{GB} for Fe3Zr. $T = 550$°C.[40] (b) Grain size vs. temperature for FeZr alloys.[40]

Model Proposed by Trelewicz and Schuh In the Weissmüller,[35,36] Kirchheim and coworkers, [37–39,51,52] and Darling et al. models,[40] various approximations are required to obtain a result in the form of Equation (1). The equilibrium grain size is determined through solute mass balance for an interfacial monolayer or bilayer grain boundary. The regular solution model [41] proposed by Trelewicz and Schuh (TS) eliminates many of the approximations in previous models, for example fully saturated grain boundaries or dilute solution approximations. The TS model as proposed does not include elastic size misfit enthalpy ΔH_{els} and this reduces the range of application to phase separation type systems, $\Delta H_{\text{chem}} > 0$. The approach evaluates the excess Gibbs mixing free energy ΔG_{mix} of a binary AB alloy system using a model where grain boundary regions and bulk regions with variable volume fractions and solute concentrations are separated by transitional bonds. ΔG_{mix} is obtained from the difference in the nearest neighbor bond energy and mixing entropy of this system relative to equivalent volumes of unmixed pure A and pure B with no grain boundary. The resulting equation describing ΔG_{mix} includes terms that in general case do not reduce to the form in Equation (1). The equilibrium state is obtained by simultaneous minimization of ΔG_{mix} with respect to variations of the solute concentration and the grain boundary volume fraction, subject to mass conservation. The solution of this system of equations will lead to an equilibrium volume fraction of grain boundary (equivalent to grain size) as a function of temperature and solute concentration for alloy systems stabilized by $\Delta H_{\text{chem}} > 0$ with $\Delta H_{\text{els}} = 0$. TS present results for parametric variations in the regular solution parameters at 1,000°C that are obtained using numerical solutions to the minimization equations. Details of the numerical solution method are not given. Results are presented mostly in the form of grain size vs. global solute content plots at the specified temperature. These are not directly comparable with grain size vs. temperature plots at different solute contents shown in previous sections (Figures 2(b) and 3(b)). Figure 4(a) shows experimental results for NiW and NiP alloys deposited at 100°C, plotted as grain size vs. solute content, compared with model predictions in Figure 4(b) using estimated values of the bulk regular solutions parameters based on Miedema's model.[53] The trends are captured by the model results, although with some deviations as discussed in [41]. It is worth noting that the TS approach assumes that there is no secondary phase formation. Accordingly, it is not intended to apply where competing secondary phase formation must be considered.

Chookajorn et al. [54,55] later proposed a modified version of the TS approach incorporating the effect of solute atomic size misfit. Using this model, a nanostructured stability map was given for tungsten alloys with respect to the enthalpy of mixing versus the enthalpy of segregation. This map shows the capacity of solutes to stabilize tungsten nanoscale grain size. Murdoch et al. [56] continued the modification of TS model to identify the conditions under which binary nanocrystalline alloy systems with positive heats of mixing are stable with respect to both grain growth and phase separation. They plotted a nanostructure stability map in terms of alloy thermodynamic parameters with three main regions: (i) No grain boundary segregation region, (ii) preferentially macroscopic phase separation region, and (iii) nanocrystalline state region stable against both grain growth and phase separation. However, as will be

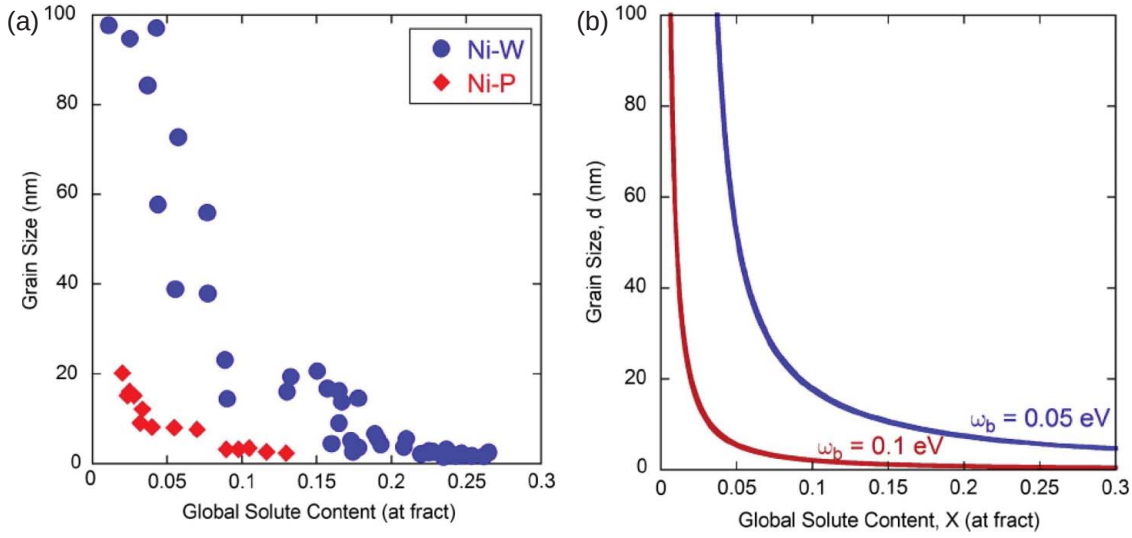

Figure 4. (a) Results obtained for $T = 100$°C.[41] (b) Model results for fitted parameters.[41]

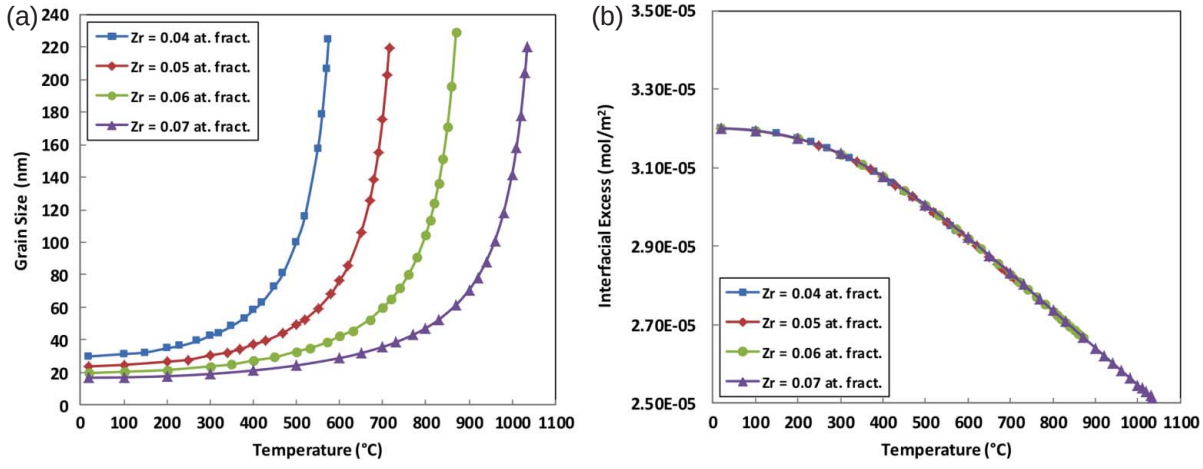

Figure 5. (a) Grain size vs. T for FeZr.[42]. (b) GB solute excess vs. T for FeZr.[42]

discussed in context with the models of Saber et al.,[42] the atomic size misfit in the modified version of this model is not properly scaled.

Modified TS Model Proposed by Saber et al. Using the TS approach for finite grain boundary and bulk regions, a regular solution model for thermodynamic stabilization of binary alloys was proposed by Saber et al. [42] using a Wynblatt–Ku approximation to incorporate both chemical and elastic enthalpy. In contrast to the original model which includes only chemical enthalpy, these authors include the elastic enthalpy as the elastic strain energy release ΔE_{els} scaled by the grain boundary region volume fraction f_{ig} and solute content x_{ig}; that is, $\Delta H_{\text{els}} = x_{\text{ig}}\, f_{\text{ig}}\, \Delta E_{\text{els}}$. This is consistent with the approach since contributions to the total mixing free energy from the bulk region and grain boundary region must be combined in proportion to their volume fractions, along with their appropriate solute contents. Including the elastic enthalpy broadens the model to a much richer range of alloy systems beyond phase separation type systems. The equilibrium condition is defined by minimization of the total Gibbs mixing free energy with respect to simultaneous variations in the solute contents and volume fractions with the constraint of overall mass balance. The Lagrange multiplier technique was used to obtain an explicit solution to the constrained equations in a form readily solved using standard numerical software packages. Results for FeZr alloys in Figure 5(a) can be compared with Darling et al. results in Figure 3(b). Both models give comparable predictions for the temperature and Zr solute concentration dependence of the metastable grain size. This implies that the dilution solution limit used for model results in Figure 3(b) is appropriate for this system. Figure 5(b) shows the corresponding grain boundary solute excess for FeZr alloys obtained with the Saber et al. model. This follows a master curve for all alloy compositions and the

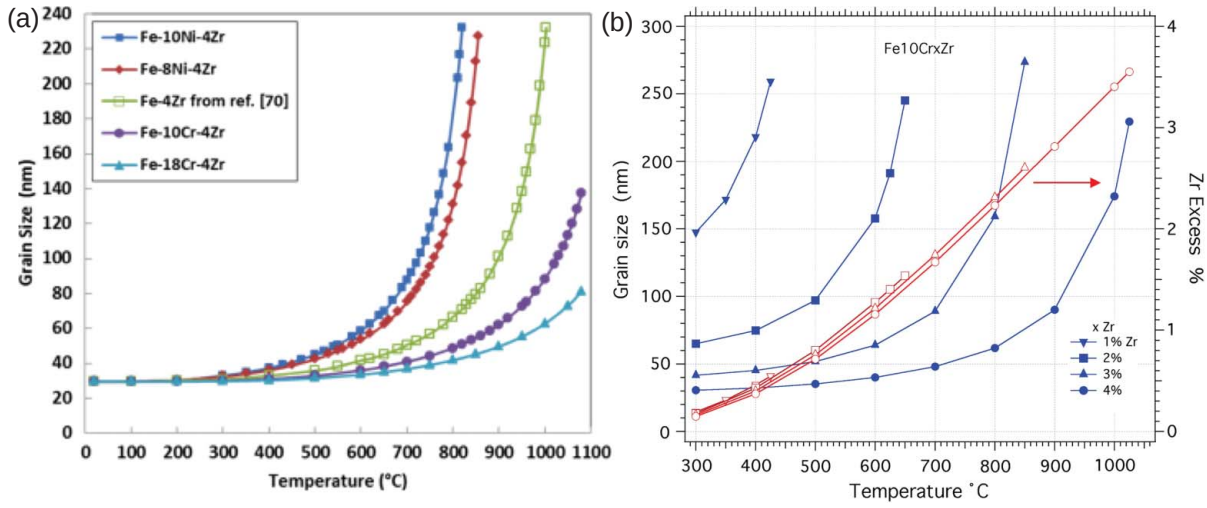

Figure 6. (a) Grain size vs. *T* for FexCr4Zr and FexNi4Zr alloys.[43] (b) Grain size and solute excess in solution for Fe10CrxZr alloys.[24]

solute excess decreases as temperature increases. The grain boundary region Zr solute content remains near 90% at 900°C.

Ternary Model Proposed by Saber et al. This was developed in [43] following the modeling approach adopted for binary alloys by these authors in [42]. The number of element pairs for binaries is 3 (AA, BB, and AB), whereas for ternaries it is 6 (AA, BB, CC, AB, AC, and BC). For binaries, one considers a pure elemental solvent A with stabilizer element B. For ternaries, one considers an AB alloy solvent with stabilizer element C. This notably expands the application space for thermodynamic stabilization of alloys, and introduces additional solute–solvent interactions that can be beneficial or detrimental. The solution for the ternary model requires simultaneous minimization of five equations with two constraint conditions. It is again obtained using the LaGrange multipliers and standard numerical routines. An example of the possible effect that additional alloying elements can have compared to the binary alloy counterpart is shown in Figure 6(a) for Fe–Ni–4Zr, Fe–Cr–4Zr, and Fe–4Zr alloys. Relative to the baseline Fe–4Zr binary alloy, it can be seen that Ni reduces the effectiveness of the thermodynamic stabilization, whereas Cr increases it. This is due to the additional bond pair interactions. It should also be noted that phase transformations have an influence on obtaining grain size stabilization, notably with Ni additions in Fe–Ni or Fe–Ni–Cr alloys.[57,58] These latter effects are not included in the thermodynamic stabilization models. Figure 6(b) shows an additional aspect of the ternary model, which is also obtained in a binary model. In addition to the grain size vs. temperature curves for Fe10CrxZr, the %Zr solute excess remaining in bulk solution at stabilization is shown (right side scale). This appears as a master curve for all alloy compositions. If this remaining bulk solute content is greater than the bulk solute content in equilibrium at a given temperature (approximately 0.2 at.% at 900°C for Zr in Fe), it will react to produce Fe–Cr–Zr intermetallic particles, and oxides or carbides if O or C contaminants are induced during BM. The solute excess remaining in grains at 900°C is 1.2% Zr in Figure 6(b) for a 90-nm grain size 4%Zr alloy. Additional precipitation reactions must be anticipated in conjunction with grain size stabilization. These effects were observed in [59]. An optimal thermodynamic stabilization scenario would therefore be obtained in alloy systems where the excess solute left in bulk solution is less than the equilibrium solute concentration at the same temperature. This adds an additional aspect to selection of appropriate stabilization solutes.

This approach, however, does not include energy changes due to the precipitate/particle formation. The excess solute remaining in the matrix can lead to precipitate formation, and drive the stabilization towards kinetic mechanisms such as the Zener pinning effect. This limitation may be considered as a relevant point for further modification of thermodynamic stabilization models.

The kinetic stabilization due to the presence of nanoscale secondary phases including intermetallic compounds and oxide particles is possible and has been reported for many alloys, for example, Al-base alloys.[60] Complete understanding and exploitation of the stabilization of nanoscale grain size at high temperatures by solute additions must take into account both thermodynamic and kinetic stabilization mechanisms, along with time–temperature paths used for processing. Atomic scale resolution for structure and chemistry of solute segregation to grain boundaries and precipitation of nanoscale phases, for example by the use of atom

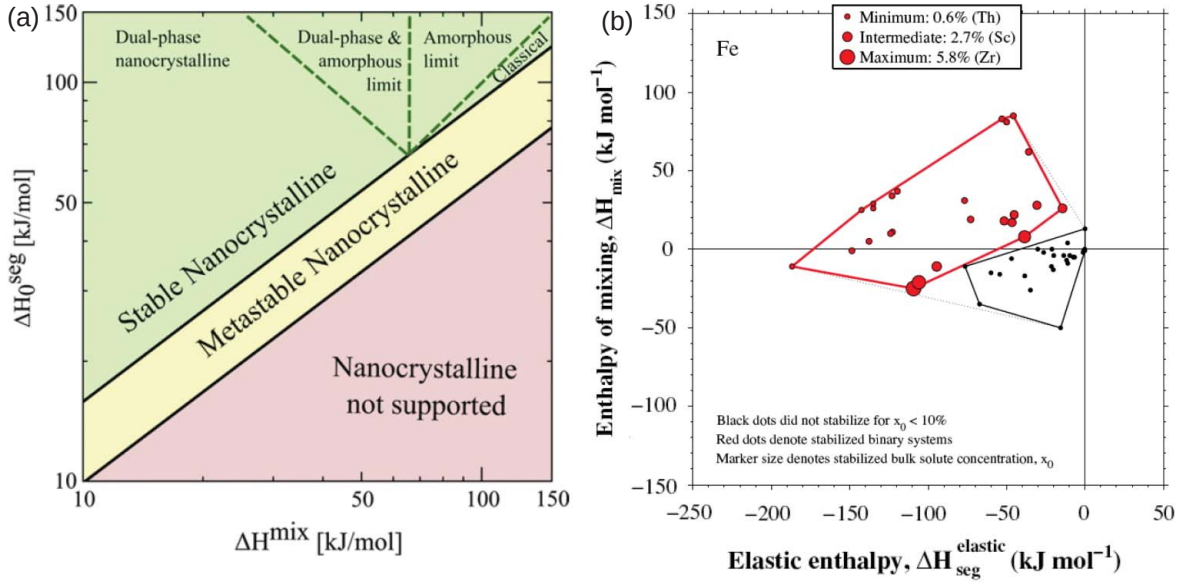

Figure 7. (a) Stability map from [56]. (b) Stability map from [40].

probe tomography or high-resolution scanning transmission electron microscopy, is necessary to confirm the relevance and interplay of thermodynamic and kinetic mechanisms.

Nanostructure Stability Maps Schuh and coworkers [54–56] proposed microstructure stability maps for thermodynamically stabilized nanocrystalline alloys at selected temperatures. These were developed for phase-separating binary systems stabilized by positive mixing enthalpy ΔH_{mix} and positive segregation enthalpy ΔH_{seg}. The latter was obtained from a segregation isotherm given in the TS model.[41] The methodology presented by Murdoch et al. [56] used results from the thermodynamic stabilization model combined with additional criteria to develop the microstructure stability map in Figure 7(a). The map plots enthalpy of segregation vs. enthalpy of mixing and shows, for example, the amorphous phase limit that would be stabilized in this region if the TS model has the absolute lowest free energy relative to other possibilities. Maps are developed for specified temperatures, and the example in Figure 7(a) is at $T = 0.35T_{\text{cr}}$, where T_{cr} is the onset of phase separation. Chookajorn et al. [54] proposed a map for W-base alloys in conjunction with experimental results for W–Ti alloys. Chookajorn et al. [61] reported Monte Carlo simulations for a range of nanoscale microstructures in conjunction with the stability map developed in [54]. Darling et al. [40] used their model in conjunction with the data compilation in [50] to include a wide range of possible solutes in selected matrices. In this case, the maps plot enthalpy of mixing vs. elastic enthalpy of segregation for different solutes in a given matrix. A map for Fe-base alloys is shown in Figure 7(b), where the size of a circle corresponds to the relative magnitude of the solute content needed for stabilization at a grain size of 25 nm at $T/T_{\text{MP}} = 0.6$. The list of solutes and related data for each solvent matrix are given in [40].

Atomistic Simulations and Modeling Related to Thermodynamic Stabilization Atomistic simulations have proved useful for investigating many aspects of nanocrystalline materials, such as plastic deformation and radiation damage. Simulations related to thermodynamic stabilization are discussed in this section. Millet et al. [62–64] used molecular statics and molecular dynamics to investigate grain boundary stabilization in a Cu binary alloy using a Lennard–Jones potential. Solute dopant atoms with various size misfit radius $\triangle r$ and interfacial excess Γ were annealed at 1,200 K by simulation. In addition to characterizing the grain boundary structural development, the simulations predicted that the excess grain boundary energy γ decreases to zero with sufficient dopant additions, as shown in Figure 8(a) for increasing size misfit radius $\triangle r$. The trend follows the results reported by Darling et al. [40] in Figure 3(a). Formation of the second phase was not considered in these simulations. In another series of papers, Purohit et al. [65–67] used MEAM and DFT calculations to investigate grain boundary segregation in AlPb alloys. A MEAM potential was developed to model the Al–Pb system.[65] Additions of Pb to Al have negative size misfit enthalpy and positive mixing enthalpy, both of which would favor grain boundary segregation, However, solute clustering (phase separation) due to the mixing enthalpy is also possible. Molecular statics models indicated that as Pb content increases, the suitable grain boundary sites are fully saturated and Pb clusters

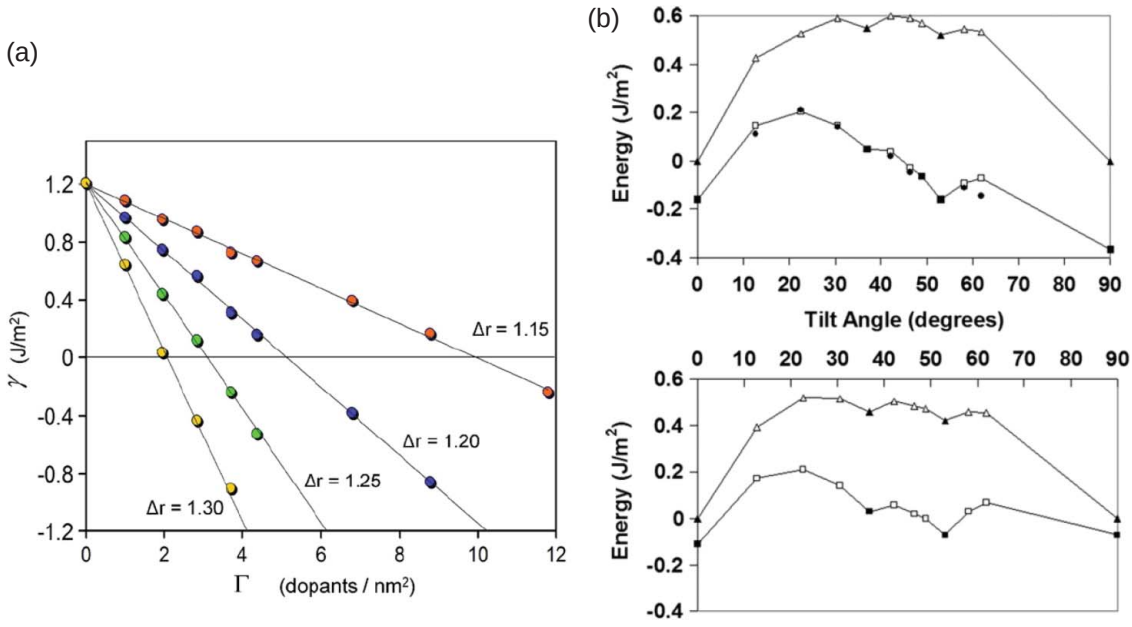

Figure 8. (a) γ vs. Γ for a range of misfit Δr.[64]. (b) γ vs. tilt angle using MEAM (upper plot) vs. DFT (lower plot) calculations.[66]

containing about 10 atoms can then nucleate, consistent with the positive mixing enthalpy [66]. Σ grain boundaries and random tilt grain boundaries in Al–Pb were modeled over the full range of tilt angles 0–90° in [67] using MEAM and DFT models in conjunction with disclination models. The upper and lower curves in each of the two frames in Figure 8(b) correspond to unsegregated and fully segregated grain boundaries, respectively. The results show that $\gamma \leq 0$ would be obtained over a significant portion of the tilt angle range, indicating that thermodynamic stabilization can be inclusive for both random and high symmetry grain boundaries. Some differences arise for MEAM (top frame) vs. DFT (bottom frame) calculations as indicated in Figure 8(b).

Kircheim [51,52] considered the problem of extending thermodynamic models for solute excess and concomitant free energy changes to include defects such as dislocations and vacancies, as well as including surfaces and interfaces. A more general definition of solute excess for defect formation energies is obtained.[52] The effects of open vs. closed systems were also treated. Applications to phenomena such as decreased vacancy formation energies, solute segregation to dislocations, solid solution softening, and hydrogen-enhanced plasticity are reviewed in conjunction with excess free energy and possible thermodynamic stabilization.[51,52]

Summary The models in this overview included analytical and numerical approaches to thermodynamic stabilization in nanocrystalline alloys. Model predictions compared with experimental results revealed that there are some cases where the predictions are in reasonable agreement with experimental observation and thermodynamic stabilization would be viable. However, there are alloy systems in which thermodynamic stabilization cannot be effective. In the Weissmüller,[35,36] Kichheim,[37,51,52] and Darling models,[40] the analytical methods evaluate thermodynamic stabilization for a system which is a dilute solution containing a negligible volume fraction of grain boundary. It must be noted that these limitations are not satisfied in a nanocrystalline microstructure where the amount of grain boundary is significant and the grain boundary solute content can be larger than that of dilute solution. In the work of Trelewicz and Schuh,[41] these limitations are eliminated. The TS model applies to thermodynamic stabilization of non-dilute systems with either weakly or strongly segregating solutes. However, the role of elastic enthalpy due to the atomic size misfit is not considered. Saber et al. [42] modified the TS approach and incorporate the release of stain energy due to atomic size misfit into the total Gibbs free energy. The numerical approach provided in the Saber et al. work predicts the thermal stability of nanoscale grain size for any combination of A and B atoms. This approach is extended to ternary alloy systems.[43] However, the effect of simultaneous precipitate formation on the total Gibbs free energy remains to be addressed in order to provide a comprehensive regular solution model for a combined stabilization mechanism.

Disclosure Statement No potential conflict of interest was reported by the authors.

Funding This work was supported by the Department of Energy [grant DE-NE0000538].

References

[1] Koch CC. Nanostructured materials: processing, properties and applications. Norwich (NY): William Andrew; 2006.

[2] Suryanarayana C. Nanocrystalline materials. Int Mater Rev. 1995;40:41–64.

[3] Gleiter H. Nanocrystalline materials. Prog Mater Sci. 1989;33:223–315.

[4] Nieman GW, Weertman JR, Siegel RW. Mechanical behavior of nanocrystalline Cu and Pd. J Mater Res. 1991;6:1012–1027.

[5] Xiao C, Mirshams RA, Whang SH, Yin WM. Tensile behavior and fracture in nickel and carbon doped nanocrystalline nickel. Mater Sci Eng A. 2001;301:35–43.

[6] Yin WM, Whang SH, Mirshams R, Xiao CH. Creep behavior of nanocrystalline nickel at 290 and 373 K. Mater Sci Eng A. 2001;301:18–22.

[7] Lu L, Li SX, Lu K. Scr Mater. 2001;45:1163.

[8] Kim HS, Hong SI, Lee YS, Dubravina AA, Alexandrov IV. Deformation behavior of copper during a high pressure torsion process. J Mater Process Technol. 2003;142:334–337.

[9] Liao XZ, Zhao YH, Srinivasan SG, Zhu YT, Valiev RZ, Gunderov DV. Deformation twinning in nanocrystalline copper at room temperature and low strain rate. Appl Phys Lett. 2004;84:592.

[10] Kawasaki M, Figueiredo RB, Langdon TG. An investigation of hardness homogeneity throughout disks processed by high-pressure torsion. Acta Mater. 2011;59:308–316.

[11] Edalati K, Fujioka T, Horita Z. Microstructure and mechanical properties of pure Cu processed by high-pressure torsion. Mater Sci Eng A. 2008;497:168–173.

[12] Wen H, Zhao Y, Li Y, Ertorer O, Nesterov KM, Islamgaliev RK, Valiev RZ, Lavernia EJ. High-pressure torsion-induced grain growth and detwinning in cryomilled Cu powders. Philos Mag. 2010;90:4541–4550.

[13] Liao XZ, Kilmametov AR, Valiev RZ, Gao H, Li X, Mukherjee AK, Bingert JF, Zhu YT. High-pressure torsion-induced grain growth in electrodeposited nanocrystalline Ni. Appl Phys Lett. 2006;88:021909.

[14] Iwahashi Y, Wang J, Horita Z, Nemoto M, Langdon TG. Principle of equal-channel angular pressing for the processing of ultra-fine grained materials. Scr Mater. 1996;35:143–146.

[15] Xu C, Furukawa M, Horita Z, Langdon TG. The evolution of homogeneity and grain refinement during equal-channel angular pressing: a model for grain refinement in ECAP. Mater Sci Eng A. 2005;398:66–76.

[16] Terhune SD, Swisher DL, Oh-Ishi K, Horita Z, Langdon TG, McNelley TR. An investigation of microstructure and grain-boundary evolution during ECA pressing of pure aluminum. Metall Mater Trans A. 2002;33:2173–2184.

[17] Sun PL, Kao PW, Chang CP. Effect of deformation route on microstructural development in aluminum processed by equal channel angular extrusion. Metall Mater Trans A. 2004;35:1359–1368.

[18] Stolyarov VV, Zhu YT, Alexandrov IV, Lowe TC, Valiev RZ. Influence of ECAP routes on the microstructure and properties of pure Ti. Mater Sci Eng A. 2001;299:59–67.

[19] Komura S, Horita Z, Nemoto M, Langdon TG. Influence of stacking fault energy on microstructural development in equal-channel angular pressing. J Mater Res. 1999;14:4044–4050.

[20] Suryanarayana C, Ivanov E, Boldyrev VV. The science and technology of mechanical alloying. Mater Sci Eng A. 2001;304–306:151–158.

[21] Koch CC, Cho YS. Nanocrystals by high energy ball milling. Nanostruct Mater. 1992;1:207–212.

[22] Koch CC. Synthesis of nanostructured materials by mechanical milling: problems and opportunities. Nanostruct Mater. 1997;9:13–22.

[23] Eckert J, Holzer JC, Krill CE, Johnson WL. Structural and thermodynamic properties of nanocrystalline fcc metals prepared by mechanical attrition. J Mater Res. 1992;7:1751–1761.

[24] Hellstern E, Fecht HJ, Fu Z, Johnson WL. Structural and thermodynamic properties of heavily mechanically deformed Ru and AlRu. J Appl Phys. 1989;65:305.

[25] Oleszak D, Shingu PH. Nanocrystalline metals prepared by low energy ball milling. J Appl Phys. 1996;79:2975.

[26] Gaffet E, Harmelin M. Crystal-amorphous phase transition induced by ball-milling in silicon. J Common Met. 1990;157:201–222.

[27] Shen TD, Koch CC, McCormick TL, Nemanich RJ, Huang JY, Huang JG. The structure and property characteristics of amorphous/nanocrystalline silicon produced by ball milling. J Mater Res. 1995;10:139–148.

[28] Shen TD, Ge WQ, Wang KY, Quan MX, Wang JT, Wei WD, Koch CC. Structural disorder and phase transformation in graphite produced by ball milling. Nanostruct Mater. 1996;7:393–399.

[29] Suryanarayana C. Mechanical alloying and milling. Prog Mater Sci. 2001;46:1–184.

[30] Darling KA, Roberts AJ, Mishin Y, Mathaudhu SN, Kecskes LJ. Grain size stabilization of nanocrystalline copper at high temperatures by alloying with tantalum. J Alloys Compd. 2013;573:142–150.

[31] Koch CC, Scattergood RO, Darling KA, Semones JE. Stabilization of nanocrystalline grain sizes by solute additions. J Mater Sci. 2008;43:7264–7272.

[32] Andrievski RA. Review of thermal stability of nanomaterials. J Mater Sci. 2014;49:1449–1460.

[33] Cahn JW. In: Johnson WC, Blakely JM, editors. Surface segregation in metals and alloys. Metals Park: ASM; 1979.

[34] Hondros ED, Seah MP. The theory of grain boundary segregation in terms of surface adsorption analogues. Metall Trans A. 1977;8:1363–1371.

[35] Weissmüller J. Alloy effects in nanostructures. Nanostruct Mater. 1993;3:261–272.

[36] Weissmüller J. Alloy thermodynamics in nanostructures. J Mater Res. 1994;9:4–7.

[37] Kirchheim R. Grain coarsening inhibited by solute segregation. Acta Mater. 2002;50:413–419.

[38] Liu F, Kirchheim R. Grain boundary saturation and grain growth. Scr Mater. 2004;51:521–525.

[39] Liu F, Kirchheim R. Nano-scale grain growth inhibited by reducing grain boundary energy through solute segregation. J Cryst Growth. 2004;264:385–391.

[40] Darling KA, Tschopp MA, VanLeeuwen BK, Atwater MA, Liu ZK. Mitigating grain growth in binary nanocrystalline alloys through solute selection based on thermodynamic stability maps. Comput. Mater. Sci. 2014;84:255–266.

[41] Trelewicz JR, Schuh CA. Grain boundary segregation and thermodynamically stable binary nanocrystalline alloys. Phys Rev B. 2009;79:094112.

[42] Saber M, Kotan H, Koch CC, Scattergood RO. Thermodynamic stabilization of nanocrystalline binary alloys. J Appl Phys. 2013;113:063515.
[43] Saber M, Kotan H, Koch CC, Scattergood RO. A predictive model for thermodynamic stability of grain size in nanocrystalline ternary alloys. J Appl Phys. 2013;114:103510.
[44] McLean D. 1957.
[45] Defay R, Bellemans A, Prigogine I. CERN Document Server; 1966.
[46] Burton JJ, Machlin ES. Prediction of segregation to alloy surfaces from bulk phase diagrams. Phys Rev Lett. 1976;37:1433.
[47] Wynblatt P, Ku RC. Surface energy and solute strain energy effects in surface segregation. Surf Sci. 1977;65: 511–531.
[48] Wynblatt P, Chatain D. Anisotropy of segregation at grain boundaries and surfaces. Metall Mater Trans A. 2006;37:2595–2620.
[49] Friedel J. Electronic structure of primary solid solutions in metals. Adv Phys. 1954;3:446–507.
[50] Atwater MA, Darling KA. A Visual Library of Stability in Binary Metallic Systems: The Stabilization of Nanocrystalline Grain Size by Solute Addition: Part 1, Army Research Laboratory; 2012.
[51] Kirchheim R. Reducing grain boundary, dislocation line and vacancy formation energies by solute segregation. I. Theoretical background. Acta Mater. 2007;55: 5129–5138.
[52] Kirchheim R. Reducing grain boundary, dislocation line and vacancy formation energies by solute segregation. II. Experimental evidence and consequences. Acta Mater. 2007;55:5139–5148.
[53] Miedema AR. On the heat of formation of solid alloys. II. J Less Common Met. 1976;46:67–83.
[54] Chookajorn T, Murdoch HA, Schuh CA. Design of stable nanocrystalline alloys. Science. 2012;337:951–954.
[55] Chookajorn T, Schuh CA. Nanoscale segregation behavior and high-temperature stability of nanocrystalline W–20 at.% Ti. Acta Mater. 2014;73:128–138.
[56] Murdoch HA, Schuh CA. Stability of binary nanocrystalline alloys against grain growth and phase separation. Acta Mater. 2013;61:2121–2132.
[57] Kotan H, Saber M, Koch CC, Scattergood RO. Effect of annealing on microstructure, grain growth, and hardness of nanocrystalline Fe–Ni alloys prepared by mechanical alloying. Mater Sci Eng A. 2012;552: 310–315.
[58] Kotan H, Darling KA, Saber M, Koch CC, Scattergood RO. Effect of zirconium on grain growth and mechanical properties of a ball-milled nanocrystalline FeNi alloy. J Alloys Compd. 2013;551:621–629.
[59] Saber M, Kotan H, Koch CC, Scattergood RO. Thermal stability of nanocrystalline Fe–Cr alloys with Zr additions. Mater Sci Eng A. 2012;556:664–670.
[60] Witkin DB, Lavernia EJ. Synthesis and mechanical behavior of nanostructured materials via cryomilling. Prog Mater Sci. 2006;51:1–60.
[61] Chookajorn T, Schuh CA. Thermodynamics of stable nanocrystalline alloys: a Monte Carlo analysis. Phys Rev B. 2014;89:064102.
[62] Millett PC, Selvam RP, Bansal S, Saxena A. Atomistic simulation of grain boundary energetics – Effects of dopants. Acta Mater. 2005;53:3671–3678.
[63] Millett PC, Selvam RP, Saxena A. Molecular dynamics simulations of grain size stabilization in nanocrystalline materials by addition of dopants. Acta Mater. 2006;54:297–303.
[64] Millett PC, Selvam RP, Saxena A. Stabilizing nanocrystalline materials with dopants. Acta Mater. 2007;55: 2329–2336.
[65] Purohit Y, Jang S, Irving DL, Padgett CW, Scattergood RO, Brenner DW. Atomistic modeling of the segregation of lead impurities to a grain boundary in an aluminum bicrystalline solid. Mater Sci Eng A. 2008;493: 97–100.
[66] Purohit Y, Sun L, Irving DL, Scattergood RO, Brenner DW. Computational study of the impurity induced reduction of grain boundary energies in nano- and bicrystalline Al–Pb alloys. Mater Sci Eng A. 2010;527: 1769–1775.
[67] Purohit Y, Sun L, Shenderova O, Scattergood RO, Brenner DW. First-principles-based mesoscale modeling of the solute-induced stabilization of ⟨100⟩ tilt grain boundaries in an Al–Pb alloy. Acta Mater. 2011;59: 7022–7028.